

UC Berkeley

UC Berkeley Previously Published Works

Title

Terahertz VRT spectroscopy of the water hexamer-d12 prism: Dramatic enhancement of bifurcation tunneling upon librational excitation

Permalink

<https://escholarship.org/uc/item/54d78524>

Journal

The Journal of Chemical Physics, 148(9)

ISSN

0021-9606

Authors

Cole, William TS
Farrell, James D
Sheikh, Akber A
[et al.](#)

Publication Date

2018-03-07

DOI



10.1063/1.5006195

Peer reviewed

Terahertz VRT spectroscopy of the water hexamer- d_{12} prism: Dramatic enhancement of bifurcation tunneling upon librational excitation

Cite as: J. Chem. Phys. **148**, 094301 (2018); <https://doi.org/10.1063/1.5006195>

Submitted: 22 September 2017 . Accepted: 12 February 2018 . Published Online: 01 March 2018

William T. S. Cole, James D. Farrell, Akber A. Sheikh, Özlem Yönder , Raymond S. Fellers, Mark R. Viant, David J. Wales , and Richard J. Saykally 



View Online



Export Citation



CrossMark

ARTICLES YOU MAY BE INTERESTED IN

Hydrogen bond network rearrangement dynamics in water clusters: Effects of intermolecular vibrational excitation on tunneling rates

The Journal of Chemical Physics **147**, 064301 (2017); <https://doi.org/10.1063/1.4997046>

Hydrogen bond breaking dynamics in the water pentamer: Terahertz VRT spectroscopy of a 20 μm libration

The Journal of Chemical Physics **146**, 014306 (2017); <https://doi.org/10.1063/1.4973418>

A consistent and accurate ab initio parametrization of density functional dispersion correction (DFT-D) for the 94 elements H-Pu

The Journal of Chemical Physics **132**, 154104 (2010); <https://doi.org/10.1063/1.3382344>

Lock-in Amplifiers

Find out more today



Zurich
Instruments



Terahertz VRT spectroscopy of the water hexamer-d₁₂ prism: Dramatic enhancement of bifurcation tunneling upon librational excitation

William T. S. Cole,¹ James D. Farrell,² Akber A. Sheikh,¹ Özlem Yönder,^{1,3} Raymond S. Fellers,^{1,a)} Mark R. Viant,^{1,b)} David J. Wales,⁴ and Richard J. Saykally^{1,c)}

¹Department of Chemistry, University of California, Berkeley, California 94720, USA

²CAS Key Laboratory of Soft Matter Physics, Beijing National Laboratory for Condensed Matter Physics, Institute of Physics, Chinese Academy of Sciences, Beijing 100190, China

³Lehrstuhl für Theoretische Chemie, Ruhr-Universität Bochum, D-44780 Bochum, North Rhine-Westphalia, Germany

⁴Department of Chemistry, University of Cambridge, Cambridge CB2 1EW, United Kingdom

(Received 22 September 2017; accepted 12 February 2018; published online 1 March 2018)

Using diode laser vibration-rotation-tunneling spectroscopy near 15 THz (500 cm⁻¹), we have measured and assigned 142 transitions to three a-type librational subbands of the water hexamer-d₁₂ prism. These subbands reveal dramatically enhanced (ca. 1000×) tunneling splittings relative to the ground state. This enhancement is in agreement with that observed for the water dimer, trimer, and pentamer in this same frequency region. The water prism tunneling motion has been predicted to potentially describe the motions of water in interfacial and confined environments; hence, the results presented here indicate that excitation of librational vibrations has a significant impact on the hydrogen bond dynamics in these macroscopic environments. *Published by AIP Publishing.* <https://doi.org/10.1063/1.5006195>

INTRODUCTION

The challenge in developing a general predictive molecular-scale description of water is essentially that of correctly describing its extended and dynamic hydrogen-bonded network.^{1–9} High-resolution spectroscopy of water clusters provides a means of systematically untangling its complexities. In this context, the water hexamer is of particular interest, as it is the smallest cluster exhibiting a 3-D hydrogen bond network.^{4,10–23} Previous studies have revealed the existence of low energy cage, prism, and book hexamer isomers within a supersonic expansion.^{12,24–27} It has been established that the cage isomeric structure is the global minimum energy structure for the all-H₂O isomer,^{12,28} although the prism isomer lies in close energetic proximity, and is actually the lowest energy isomer for the all-D₂O isomer.^{4,25,28–36} Additionally, cyclic hexamer clusters have been observed in frozen rare gas matrices.^{37,38}

The first detailed experimental study of a water hexamer cluster was reported by Liu *et al.*, who observed and characterized terahertz spectra of the cage isomer in a supersonic expansion.^{12,24} More recently, Perez *et al.* observed the cage, prism, and book isomers (in addition to heptamer and nonamer clusters) in a supersonic expansion using broadband microwave spectroscopy.^{25,39} This study characterized the ground state

structures of these isomers at high resolution and provided critical insights into the associated hydrogen bond network tunneling motions. A subsequent study by Richardson *et al.* provided an in-depth description of the tunneling motions of the prism, revealing a pathway which simultaneously breaks two hydrogen bonds.²⁶ The structure of the water prism is shown in Fig. 1.

Here we report the measurement of a parallel vibration-rotation-tunneling (VRT) librational band of a (D₂O)₆ cluster centered in the 15 THz (510 cm⁻¹) region. The experimental rotational constants describing the mass distribution in the cluster via the principal moments of inertia extracted from the present VRT spectra agree most closely with those predicted for the prism structure. We find a dramatic librational enhancement in the bifurcation tunneling splittings of the D₂O cluster relative to the ground state, in analogy with other recent cluster studies in this spectral region.^{40–44}

EXPERIMENTAL

Our previous investigations of water dimer, trimer, and pentamer librational motions in the 15 THz region prompted us to search for similar transitions in larger clusters.^{43,45} The Berkeley diode laser/supersonic beam spectrometer used in this study has been described in detail elsewhere and only a short description is provided here.^{46,47}

A helium-cooled spectrometer (Spectra Physics) using lead-salt diodes (Laser Photonics) was used to produce infrared radiation from 509 to 514 cm⁻¹. The beam was multipassed 18–22 times through a pulsed planar supersonic expansion of a mixture of D₂O and He using a Herriott cell and detected

^{a)}Present address: Picarro, 3105 Patrick Henry Drive, Santa Clara, California 95054, USA.

^{b)}Present address: School of Biosciences, University of Birmingham, Edgbaston, Birmingham B15 2TT, United Kingdom.

^{c)}Author to whom correspondence should be addressed: saykally@berkeley.edu

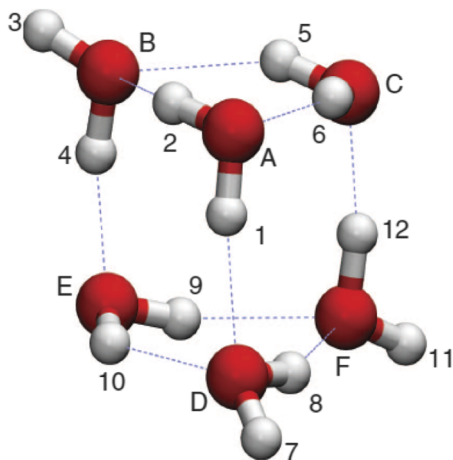


FIG. 1. The lowest energy structure of the water hexamer prism. Oxygens are labeled as A–F, and hydrogens are labeled as 1–12. Reproduced with permission from Richardson *et al.*, *Science* **351**, 1310 (2016). Copyright 2016 AAAS.

using a helium-cooled (Si:B) photoconductive detector (IR Labs). The supersonic expansion was produced by bubbling pure He gas, with a backing pressure of 1–2 atm through liquid D₂O (Cambridge Labs, 99.96% purity), and then expanding through a 101.6 mm long slit at a repetition rate of 35 Hz into a vacuum chamber maintained at \sim 200 mTorr by a Roots blower (Edwards 4200) backed by two rotary pumps

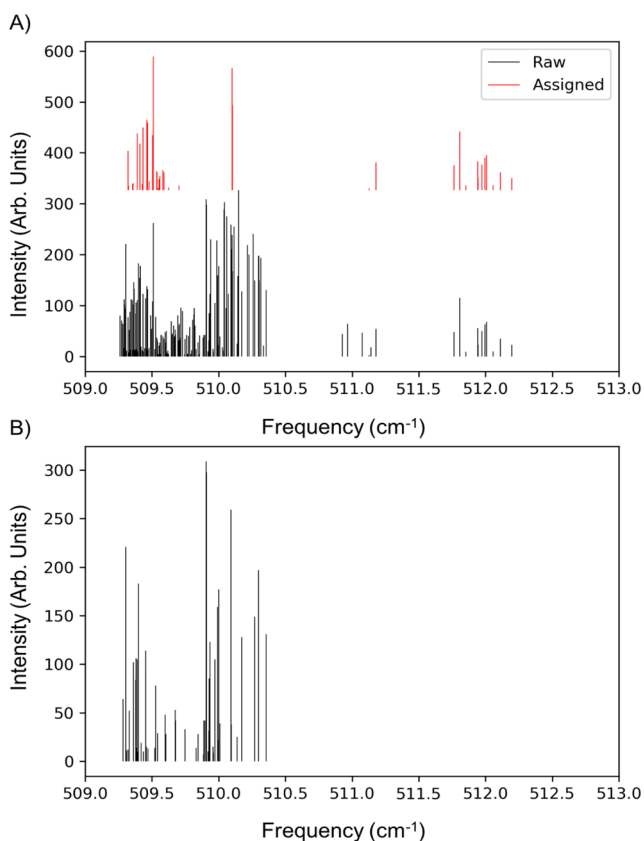


FIG. 2. (a) All 188 transitions observed in the experimental range examined are shown in black. The 46 remaining unassigned transitions are shown in red. (b) Transitions assigned to subband 3, showing the typical pattern observed in these experiments. Laser gaps prohibited further assignment of the R and P branches.

(E2M 275).⁴⁸ Simultaneously, the fringe spacing of a vacuum-spaced etalon and carbonyl sulfide (OCS) reference gas spectra was detected with a liquid He cooled (Cu:Ge) detector (Santa Barbara Research Center) and recorded to enable precise frequency calibration. The observed linewidths of \sim 30–40 MHz full-width half maximum (FWHM) are somewhat larger than the Doppler-limited linewidths extrapolated from earlier experiments using argon expansions. Typical frequency measurement accuracy is 10–20 MHz, limited by both linewidths of the cluster absorptions and laser drift. Spectra were detected in direct absorption using a time-gated phase sensitive signal processing approach.⁴⁸

Accessing the 15 THz (500 cm^{-1}) region of the electromagnetic spectrum has generally been notoriously difficult. The spectra reported here required the use of 10 separate laser diodes, each scanned across several modes to cover the specified spectral range. Moreover, large laser gaps are present in the spectra, which causes considerable difficulty in the assignment. Additionally, the spectrum reflects several distinct laser intensity fluctuations across different devices that are apparent in the complete spectra shown in Fig. 2. Specifically, between 512.4 cm^{-1} and 513.2 cm^{-1} the laser intensity is enhanced (as was found in a previous study⁴¹) and between 509.5 cm^{-1} and 510 cm^{-1} the laser intensity is depressed.

RESULTS AND ANALYSIS

Assignment

We have assigned 142 of the 188 observed transitions in the studied region using the PGOPHER platform.⁴⁹ The transitions belong to three distinct a-type ($\Delta K_a = 0$) subbands, which are assigned to different tunneling levels of the water hexamer-d₁₂ prism isomer. The observed transitions were fit to an S-reduced Watson Hamiltonian. For the assignment, we fixed the ground state constants to those obtained in Ref. 44. Correlation matrices of the fit and a list of all assigned transitions are given in the [supplementary material](#).

Anharmonic excited state vibrational calculations

To elucidate the nature of the observed vibration, anharmonic frequencies and rotational constants were calculated by applying generalized second-order vibrational perturbation theory (GVPT2)^{50,51} to the second-order Møller–Plesset (MP2) perturbation theory potential energy surface using the Gaussian 09 D.01 package.⁵² The geometry of the lowest energy D₂O prism was optimized at the MP2/aug-cc-pVDZ level of theory enforcing “very tight” convergence criteria, following which a GVPT2 calculation was performed at the same level of theory using the parameters recommended by Temelso and Shields.²³ The Gaussian input file, the full list of calculated harmonic and anharmonic frequencies, and the rotational constants are listed in the [supplementary material](#).

Fit analysis

We obtained a good quality fit of the observed transitions; the average RMS of the fit is \sim 37 MHz as a result of the wavelength accuracy of $<$ 20 MHz and the observed linewidths of 30–40 MHz (Table I). We note that the A, B, and C constants

TABLE I. Molecular constants for the asymmetric top fit with fixed ground state constants. The uncertainty in the final two digits for each constant is given in parentheses. The values of the subband origin, A, B, C, and RMS error are given in MHz; all other values are in kHz. Ground state constants were kept fixed in the fit and obtained from Ref. 44.

	Fit constants			
	Subband 1	Subband 2	Subband 3	Ground state
Origin	152 774 46(17)	152 811 36(17)	152 843 28(16)	0
A	1599.33(20)	1601.84(28)	1594.04(24)	1493.9052(12)
B	1257.40(25)	1251.51(56)	1250.01(41)	1218.3566(12)
C	1212.30(26)	1203.86(58)	1214.47(38)	1185.6460(11)
D_K	0.724(15)	-0.466(22)	-0.312(134)	$-0.961(63) \times 10^3$
D_{JK}	-0.697(11)	0.307(27)	-0.045(20)	$1.662(58) \times 10^3$
D_J	0.2245(44)	0.0103(87)	0.0476(82)	$0.4094(94) \times 10^3$
δ_K	0.593(32)	3.005(25)	2.521(97)	$-2.92(27) \times 10^3$
δ_J	0.0295(15)	0.0140(97)	-0.0664(46)	$0.0511(63) \times 10^3$
H_K	0.0210(27)	0.1283(20)	0.0769(95)	0
H_{KJ}	-0.0136(30)	-0.1843(30)	-0.1224(14)	0
H_{JK}	$-7.7(10) \times 10^4$	0.059(12)	0.0452(54)	0
H_J	$1.72(31) \times 10^3$	$-9.1(11) \times 10^4$	$-2.19(86) \times 10^3$	0
RMS (MHz)		39.2	31.0	40.3
Number of transitions		51	38	53

of all three bands show good agreement with one another, providing evidence that these bands originate from tunneling sublevels of a common excited state. Additionally, a fit with floating ground state constants yielded good agreement with the observed values from Ref. 44, although we have chosen to keep those values fixed in the reported fit.

Tunneling dynamics

We refer the reader to the recent work of Richardson *et al.* for a detailed treatment of the water hexamer prism tunneling dynamics and instead focus only on the relevant considerations for the fully deuterated cluster.²⁶ The feasible prism tunneling motions can be described by the complete nuclear permutation inversion (CNPI) subgroup isomorphic to point group D_{2d} . Previous work has shown that the water hexamer prism exhibits two feasible tunneling motions (here we define “feasible” as “experimentally observed”⁵³), which are referred to as P_a and P_g . In the CNPI notation, $P_a = (A D)(B F)(C E)(1 7)(2 8)(3 11)(4 12)(5 9)(6 10)$, where the labels correspond to the structure in Fig. 1. The motion associated with this element involves a double flip of the free hydrogens, resulting in breaking a single hydrogen bond. Likewise, in the CNPI notation, $P_g = (A D)(B F)(C E)(1 8 2 7)(3 11)(4 12)(5 9)(6 10)$, and the motion is described as a double flip accompanied by a bifurcation, which breaks two hydrogen bonds. The character table for this group is given in Table II.

The character representation of the nuclear spin wavefunction (Γ_{ns}) and the electric dipole moment (Γ_{dip}) is given at the bottom of Table II. We can reduce Γ_{ns} to its irreducible representation: $118\ 341\ A_1 \oplus 29\ 403\ A_2 \oplus 29\ 646\ B_1 \oplus 117\ 855\ B_2 \oplus 118\ 098\ E$.

For the fully deuterated hexamer prism, the total spin wavefunction must transform as A_1 which leads to the spin statistical weights: $A_1:A_2:B_1:B_2:E$ of 487:121:122:485:486. The irreducible representation of the electric dipole moment

is $A_1 \oplus 2B_2$ and for a-type ($\Delta K_a = 0$) transitions, the dipole transforms as B_2 . Thus, the expected selection rules are $A_1 \leftrightarrow B_2$, $A_2 \leftrightarrow B_1$, and $E \leftrightarrow E$. These selection rules lead to a “doublet of triplets” pattern with a central doublet, as shown in Fig. 3. Richardson *et al.* established that the energy level pattern of the hexamer prism is represented by the eigenvalue of the tunneling matrix shown in Fig. 3(a).²⁶

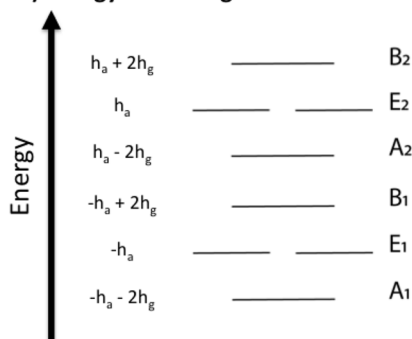
Based on these considerations, we assign the $B_2 \rightarrow A_1$, $E_2 \rightarrow E_1$, and $A_2 \rightarrow B_1$ transitions to the subbands 1, 2, and 3, respectively. This assignment is based on the equal spacing between three subbands and the intensity ratio of 1:1:0.85. While this intensity ratio does not agree quantitatively with the expected ratio (based on spin statistics above), given the large intensity fluctuations of the lasers used, we consider this assignment as the most likely of those possible under parallel selection rules. Based on this assignment, we can estimate the tunneling matrix element, h_g . The separation between subband 1 and subband 2 corresponds to the quantity $2h_g' + 2h_g''$, wherein the prime and double prime represent the values in the excited and ground state, respectively. The separation between subbands 2 and 3 corresponds to the same quantity. Given the measured values in the ground state (which are <1 MHz),

TABLE II. Character table for the point group D_{2d} ; group elements correspond to CNPI operations.

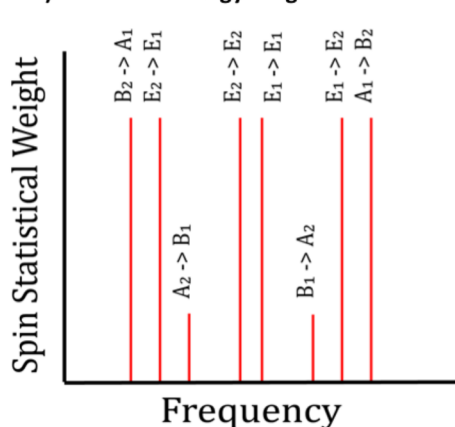
D_{2d}	E	$2P_g$	(12)(78)	$2P_a$	2(12)
A_1	1	1	1	1	1
A_2	1	1	1	-1	-1
B_1	1	-1	1	1	-1
B_2	1	-1	1	-1	1
E	2	0	-2	0	0
Γ_{ns}	531 441	243	59 049	729	177 147
Γ_{dip}	3	-1	3	-1	3

A) Tunneling Hamiltonian

$$\hat{H} = \begin{pmatrix} v & h_g & 0 & h_g & h_a & 0 & 0 & 0 \\ h_g & v & h_g & 0 & 0 & h_a & 0 & 0 \\ 0 & h_g & v & h_g & 0 & 0 & h_a & 0 \\ h_g & 0 & h_g & v & 0 & 0 & 0 & h_a \\ h_a & 0 & 0 & 0 & v & h_g & 0 & h_g \\ 0 & h_a & 0 & 0 & h_g & v & h_g & 0 \\ 0 & 0 & h_a & 0 & 0 & h_g & v & h_g \\ 0 & 0 & 0 & h_a & h_g & 0 & h_g & v \end{pmatrix}$$

B) Energy Level Diagram**C) Transitions Energy Levels**

$$\begin{aligned} B_2 \rightarrow A_1 &: E(J,K) - h_a' - h_a'' - 2h_g' - 2h_g'' \\ E_2 \rightarrow E_1 &: E(J,K) - h_a' - h_a'' \\ A_2 \rightarrow B_1 &: E(J,K) - h_a' - h_a'' + 2h_g' + 2h_g'' \\ E_2 \rightarrow E_2 &: E(J,K) + h_a' - h_a'' \\ E_1 \rightarrow E_1 &: E(J,K) - h_a' + h_a'' \\ B_1 \rightarrow A_1 &: E(J,K) + h_a' + h_a'' - 2h_g' - 2h_g'' \\ E_1 \rightarrow E_2 &: E(J,K) + h_a' + h_a'' \\ A_1 \rightarrow B_2 &: E(J,K) + h_a' + h_a'' + 2h_g' + 2h_g'' \end{aligned}$$

D) Transition Energy Diagram

we can explicitly calculate the value for the excited state (assuming these transitions originate in the ground vibrational state). Based on our fitted values of the band origins, we find the average value of h_g' to be ~ 1720 MHz, which corresponds to a ca. $1000\times$ enhancement of that tunneling splitting relative to the value for the ground state. This enhancement would be consistent with the enhancement of tunneling splitting observed for the water dimer, trimer, and pentamer upon excitation of a single quantum of 15 THz librational vibrations. We note that using the intensity ratio to assign the observed subbands to the lower triplet is in some ways arbitrary due to the power fluctuations of the diode laser. It can be argued that the subbands could be assigned to the upper triplet just as easily; however, that assignment does not change the analysis of the tunneling enhancement, as both triplets are symmetric. Further experiments are needed to definitively establish which triplet these subbands represent.

DISCUSSION**Vibrational origin**

These experiments were conducted in a He supersonic expansion, which cools the rotational temperature to approximately 10 K and the vibrational temperature to ca. 100 K. The most likely vibrational origin of the transitions is the ground state. Based on the calculated anharmonic vibrational frequencies and assuming that the transitions observed originate from the absolute ground state, we attempted to assign a vibrational mode to the experimental transitions; however, we note

several interesting observations. We find two likely candidates for anharmonic vibrational modes with transition frequencies from the absolute ground state of 505.693 and 539.359 cm^{-1} , both of which lie close to the observed average band origin of 509.7183 cm^{-1} . However, we stress that this experimental band origin corresponds to the average origin of individual tunneling bands and is not the true vibrational band origin. In Table III, we show a comparison between the observed rotational constants and the predicted values for the 4 closest vibrational modes.

From the table we can see that the observed values are all larger in magnitude than the predicted values. The most striking observation in the calculations is that the calculated values of ΔM (where M is A, B, or C) are opposite in sign and about an order of magnitude smaller than what is observed experimentally. Some of that disagreement can be attributed to the fact that there are large perturbations to the excited state, shown by the large higher order terms in the fit results, indicating a very “floppy” excited state. We have previously observed dramatic fluctuations of the centrifugal distortion constants in this experimental region.^{41,43,45} Another possibility would be that the ground state of these transitions is not actually the absolute ground state of this cluster, but rather a “hot band.” While this is unlikely, given the strong cooling in a supersonic expansion, there are several vibrational states located within 10 cm^{-1} of the absolute ground state. However, further experimental studies and calculations will be needed to determine a definitive resolution of this disagreement. We also stress that these values represent only the lower triplet of the tunneling pattern, which should be fairly representative of the excited state.

FIG. 3. (a) Tunneling Hamiltonian of the water hexamer prism. The term v represents the band origin. The terms h_g and h_a represent the tunneling splittings associated with the group elements P_g and P_a , respectively. (b) Energy level diagram resulting from the two feasible tunneling motions present in the water prism hexamer [n.b. the subscript on the E symmetry labels merely corresponds to whether the level belongs to the upper (2) or lower (1) triplet]. (c) Energies of the selection rule-allowed tunneling transitions for the prism hexamer. $E(J, K)$ represents the typical rigid rotor energy level. (N.B. E_1 and E_2 energy levels refer to whether the level belongs to the upper or lower energy triplet.) (d) Energy level diagram depicting the level ordering shown in (b). The diagram assumes that all tunneling elements are positive and $h_g' < h_g''$, which was an arbitrary choice for the figure.

TABLE III. Comparison of observed and calculated values of D₂O hexamer prism rotational constants. All values are reported in cm⁻¹.

	Origin	A	B	C	ΔA	ΔB	ΔC
Observed	509.718	0.049 831	0.041 795	0.040 368	0.003 486	0.001 155	0.000 819
Calculated	635.026	0.049 008	0.040 504	0.039 004	-0.000 141	-0.000 202	-0.000 125
	539.359	0.049 009	0.040 609	0.038 967	-0.000 140	-0.000 097	-0.000 162
	505.693	0.049 097	0.040 533	0.039 039	-0.000 052	-0.000 173	-0.000 090
	426.105	0.049 251	0.040 520	0.039 026	0.000 102	-0.000 186	-0.000 103

Librational enhancement of tunneling

We have previously studied the water dimer, trimer, and pentamer in the 15 THz librational region, with the most salient observation being the dramatic enhancement of the tunneling splittings in these clusters.^{40,41,43} We observe a similar effect here; however, we can only determine the enhancement for the h_g pathway. As described by Richardson *et al.*,²⁶ the h_g pathway motions are characterized by a double flip accompanied by a bifurcation, which involves the breaking of two hydrogen bonds. Studies of the water dimer, trimer, and pentamer tunneling in the 500 cm⁻¹ region involve motions which only break a single hydrogen bond.^{40,41,43} We observe a 1000× enhancement relative to the observed ground state tunneling for the (D₂O)₆ prism from microwave experiments.²⁶ This observation indicates that the observed enhancement in the librational region does not seem to be influenced by the number of hydrogen bonds broken in the tunneling pathway. Additionally, the reported enhancement is with respect to the observed tunneling in the (H₂O)₆ prism reported by Richardson *et al.*²⁶ As observations of the tunneling in the fully deuterated ground state do not presently exist, an accurate measure of the enhancement cannot be obtained; however, due to the larger mass-weighted path for the deuterated species, we can consider the observed 1000× enhancement as a lower bound.

Due to the absence of the higher energy triplet [Fig. 3(c)] in our measured spectra, we cannot presently characterize the h_a tunneling pathway in this excited librational state. The absence of this triplet is most likely a result of the large laser gaps present in the experiment, coupled with the fact that the observed transitions occur near the edge of the available laser coverage.

The results reported here are significant, as the water hexamer represents a transition of the minimum energy structure of water clusters from ring-like forms to a fully 3-D structure. The water prism tunneling motion has been predicted to potentially describe the motions of water in interfacial and confined environments; hence, the results presented here indicate that excitation of librational vibrations has a significant impact on the hydrogen bond dynamics in these macroscopic environments.

CONCLUSIONS

We have measured 3 a-type subbands belonging to a common librational vibration of the (D₂O)₆ prism cluster. Assigning the transitions to tunneling sublevels allows us to extract a value of ~1720 MHz for the h_g tunneling motion,

representing a ca. 1000× enhancement of the tunneling splitting, relative to the ground state splitting observed for the (H₂O)₆ cluster. This enhancement is consistent with the dramatic tunneling enhancement observed previously for the water dimer, trimer, and pentamer in the same (15 THz) experimental region.

From comparison to theoretical calculations, we find the observed change in the all-rotational constants to be dramatically larger than predicted. This large change indicates a very “floppy” excited state, which would be consistent with the large tunneling splittings observed and the breaking of one or two hydrogen bonds in the tunneling pathway.

SUPPLEMENTARY MATERIAL

See [supplementary material](#) for a list of all the assigned transitions in Table S1 and correlation matrices for the fits in Table S2. Calculated anharmonic vibrational frequencies are given in Table S3. The Gaussian input file for calculations is given in Fig. S1.

ACKNOWLEDGMENTS

The Berkeley Terahertz project was previously supported by the Chemical Structure, Dynamics, and Mechanisms-A Division of the National Science Foundation under Grant No. 1300723. This project is currently supported by the CALSOLV collaboration, an affiliate program of RESOLV (Ruhr-Universität Bochum). D.J.W. gratefully acknowledges financial support from the EPSRC.

¹D. C. Clary, “Quantum dynamics in the smallest water droplet,” *Science* **351**, 1267 (2016).

²F. N. Keutsch and R. J. Saykally, “Water clusters: Untangling the mysteries of the liquid, one molecule at a time,” *Proc. Natl. Acad. Sci. U. S. A.* **98**, 10533 (2001).

³A. Mukhopadhyay, W. T. S. Cole, and R. J. Saykally, “The water dimer. I: Experimental characterization,” *Chem. Phys. Lett.* **633**, 13 (2015).

⁴V. Babin and F. Paesani, “The curious case of the water hexamer: Cage vs. prism,” *Chem. Phys. Lett.* **580**, 1 (2013).

⁵F. Paesani, “Getting the right answers for the right reasons: Toward predictive molecular simulations of water with many-body potential energy functions,” *Acc. Chem. Res.* **49**, 1844 (2016).

⁶W. T. S. Cole, J. D. Farrell, D. J. Wales, and R. J. Saykally, “Structure and torsional dynamics of the water octamer from THz laser spectroscopy near 215 μm,” *Science* **352**, 1194 (2016).

⁷S. S. Xantheas, “*Ab initio* studies of cyclic water clusters (H₂O)_n, n = 1–6. II. Analysis of many-body interactions,” *J. Chem. Phys.* **100**, 7523 (1994).

⁸S. S. Xantheas, “*Ab initio* studies of cyclic water clusters (H₂O)_n, n = 1–6. III. Comparison of density functional with MP2 results,” *J. Chem. Phys.* **102**, 4505 (1995).

- ⁹S. S. Xantheas and T. H. Dunning, “*Ab initio* studies of cyclic water clusters (H_2O)_n, n = 1–6. I. Optimal structures and vibrational spectra,” *J. Chem. Phys.* **99**, 8774 (1993).
- ¹⁰S. E. Brown, A. W. Gotz, X. Cheng, R. P. Steele, V. A. Mandelsham, and F. Paesani, “Monitoring water clusters ‘melt’ through vibrational spectroscopy,” *J. Am. Chem. Soc.* **139**, 7082 (2017).
- ¹¹Y. Huang, X. Zhang, Z. Ma, Y. Zhou, W. Zheng, J. Zhou, and C. Q. Sun, “Hydrogen-bond relaxation dynamics: Resolving mysteries of water ice,” *Coord. Chem. Rev.* **285**, 109 (2015).
- ¹²K. Liu, M. G. Brown, C. Carter, R. J. Saykally, J. K. Gregory, and D. C. Clary, “Characterization of a cage form of the water hexamer,” *Nature* **381**, 501 (1996).
- ¹³C. H. Pham, S. K. Reddy, K. Chen, C. Knight, and F. Paesani, “Many-body interactions in ice,” *J. Chem. Theory Comput.* **13**, 1778 (2017).
- ¹⁴R. J. Saykally and D. J. Wales, “Pinning down the water hexamer,” *Science* **336**, 814 (2012).
- ¹⁵J. M. Guevara-Vela, E. Romero-Montalvo, V. A. Mora Gomez, R. Chavez-Calvillo, M. Garcia-Revilla, E. Francisco, A. M. Pendas, and T. Rocha-Rinza, “Hydrogen bond cooperativity and anticooperativity within the water hexamer,” *Phys. Chem. Chem. Phys.* **18**, 19557 (2016).
- ¹⁶M. Losada and S. Leutwyler, “Water hexamer clusters: Structures, energies, and predicted mid-infrared spectra,” *J. Chem. Phys.* **117**, 2003 (2002).
- ¹⁷C. J. Tainter, Y. Ni, L. Shi, and J. L. Skinner, “Hydrogen bonding and OH-stretch spectroscopy in water: Hexamer (cage), liquid surface, liquid, and ice,” *J. Phys. Chem. Lett.* **4**, 12 (2013).
- ¹⁸C. J. Tainter and J. L. Skinner, “The water hexamer: Three-body interactions, structures, energetics, and OH-stretch spectroscopy at finite temperature,” *J. Chem. Phys.* **137**, 104304 (2012).
- ¹⁹Y. Wang and J. M. Bowman, “IR spectra of the water hexamer: Theory, with inclusion of the monomer bend overtone, and experiment are in agreement,” *J. Phys. Chem. Lett.* **4**, 1104 (2013).
- ²⁰E. S. Kryachko, “*Ab initio* studies of the conformations of water hexamer: Modelling the penta-coordinated hydrogen-bonded pattern in liquid water,” *Chem. Phys. Lett.* **314**, 353 (1999).
- ²¹A. K. Samanta, Y. Wang, J. S. Mancini, J. M. Bowman, and H. Reisler, “Energetics and predissociation dynamics of small water, HCl, and mixed HCl-water clusters,” *Chem. Rev.* **116**, 4913 (2016).
- ²²B. Santra, A. Michaelides, M. Fuchs, A. Tkatchenko, C. Filippi, and M. Scheffler, “On the accuracy of density-functional theory exchange-correlation functionals for H bonds in small water clusters. II. The water hexamer and van der Waals interactions,” *J. Chem. Phys.* **129**, 194111 (2008).
- ²³B. Temelso and G. C. Shields, “The role of anharmonicity in hydrogen-bonded systems: The case of water clusters,” *J. Chem. Theory Comput.* **7**, 2804 (2011).
- ²⁴K. Liu, M. G. Brown, and R. J. Saykally, “Terahertz laser vibration–rotation tunneling spectroscopy and dipole moment of a cage form of the water hexamer,” *J. Phys. Chem. A* **101**, 8995 (1997).
- ²⁵C. Perez, M. T. Muckle, D. P. Zaleski, N. A. Seifert, B. Temelso, G. C. Shields, Z. Kisiel, and B. H. Pate, “Structures of cage, prism, and book isomers of water hexamer from broadband rotational spectroscopy,” *Science* **336**, 897 (2012).
- ²⁶J. O. Richardson, C. Perez, S. Lobsiger, A. A. Reid, B. Temelso, G. C. Shields, Z. Kisiel, D. J. Wales, B. H. Pate, and S. C. Althorpe, “Concerted hydrogen-bond breaking by quantum tunneling in the water hexamer prism,” *Science* **351**, 1310 (2016).
- ²⁷J. K. Gregory, D. C. Clary, K. Liu, M. G. Brown, and R. J. Saykally, “The water dipole moment in water clusters,” *Science* **275**, 814 (1997).
- ²⁸Y. Wang, V. Babin, J. M. Bowman, and F. Paesani, “The water hexamer: Cage, prism, or both. Full dimensional quantum simulations say both,” *J. Am. Chem. Soc.* **134**, 11116 (2012).
- ²⁹D. M. Bates and G. S. Tschumper, “CCSD(T) complete basis set limit relative energies for low-lying water hexamer structures,” *J. Phys. Chem. A* **113**, 3555 (2009).
- ³⁰M. Head-Gordon and T. Head-Gordon, “Analytic MP2 Frequencies without fifth-order storage. Theory and application to bifurcated hydrogen bonds in the water hexamer,” *Chem. Phys. Lett.* **220**, 122 (1994).
- ³¹J. Kim and K. S. Kim, “Structures, binding energies, and spectra of isoenergetic water hexamer clusters: Extensive *ab initio* studies,” *J. Chem. Phys.* **109**, 5886 (1998).
- ³²K. Kim, K. D. Jordan, and T. S. Zwier, “Low-energy structures and vibrational frequencies of the water hexamer: Comparison with benzene- $(\text{H}_2\text{O})_6$,” *J. Am. Chem. Soc.* **116**, 11568 (1994).
- ³³J. K. Gregory and D. C. Clary, “Theoretical study of the cage water hexamer structure,” *J. Phys. Chem. A* **101**, 6813 (1997).
- ³⁴C. Lee, H. Chen, and G. Fitzgerald, “Structures of the water hexamer using density functional methods,” *J. Chem. Phys.* **101**, 4472 (1994).
- ³⁵B. J. Mhin, H. S. Kim, H. S. Kim, C. W. Yoon, and K. S. Kim, “*Ab initio* studies of the water hexamer: Near degenerate structures,” *Chem. Phys. Lett.* **176**, 41 (1991).
- ³⁶Y. Chen and H. Li, “Intermolecular interaction in water hexamer,” *J. Phys. Chem. A* **114**, 11719 (2010).
- ³⁷S. Hirabayashi and K. M. T. Yamada, “The monocyclic water hexamer detected in neon matrices by infrared spectroscopy,” *Chem. Phys. Lett.* **435**, 74 (2007).
- ³⁸K. Nauta and R. E. Miller, “formation of cyclic water hexamer in liquid helium: The smallest piece of ice,” *Science* **287**, 293 (2000).
- ³⁹C. Perez, D. P. Zaleski, N. A. Seifert, B. Temelso, G. C. Shields, Z. Kisiel, and B. H. Pate, “Hydrogen bond cooperativity and the three-dimensional structures of water nonamers and decamers,” *Angew. Chem., Int. Ed. Engl.* **53**, 14368 (2014).
- ⁴⁰W. T. S. Cole, R. S. Fellers, M. R. Viant, C. Leforestier, and R. J. Saykally, “Far-infrared VRT spectroscopy of the water dimer: Characterization of the 20 μm out-of-plane librational vibration,” *J. Chem. Phys.* **143**, 154306 (2015).
- ⁴¹W. T. S. Cole, R. S. Fellers, M. R. Viant, and R. J. Saykally, “Hydrogen bond breaking dynamics in the water pentamer: Terahertz VRT spectroscopy of a 20 μm libration,” *J. Chem. Phys.* **146**, 014306 (2017).
- ⁴²F. N. Keutsch, R. S. Fellers, M. G. Brown, M. R. Viant, P. B. Petersen, and R. J. Saykally, “Hydrogen bond breaking dynamics of the water trimer in the translational and librational band region of liquid water,” *J. Am. Chem. Soc.* **123**, 5938 (2001).
- ⁴³F. N. Keutsch, R. S. Fellers, M. R. Viant, and R. J. Saykally, “Far-infrared laser vibration–rotation–tunneling spectroscopy of water clusters in the librational band region of liquid water,” *J. Chem. Phys.* **114**, 4005 (2001).
- ⁴⁴L. Evangelisti, C. Perez, S. Lobsiger, N. A. Seifert, D. P. Zaleski, B. H. Pate, Z. Kisiel, B. Temelso, and G. C. Shields, “Deuterated water hexamer observed by chirped-pulse rotational spectroscopy,” in International Symposium on Molecular Spectroscopy, Urbana, IL, 2014.
- ⁴⁵W. T. S. Cole and R. J. Saykally, “Hydrogen bond network rearrangement dynamics in water clusters: Effects of intermolecular vibrational excitation on tunneling rates,” *J. Chem. Phys.* **147**, 064301 (2017).
- ⁴⁶G. A. Blake, K. B. Laughlin, R. C. Cohen, K. L. Busarow, D. H. Gwo, C. A. Schmuttenmaer, D. W. Steyert, and R. J. Saykally, “Tunable far infrared laser spectrometers,” *Rev. Sci. Instrum.* **62**, 1693 (1991).
- ⁴⁷G. A. Blake, K. B. Laughlin, R. C. Cohen, K. L. Busarow, D. H. Gwo, C. A. Schmuttenmaer, D. W. Steyert, and R. J. Saykally, “The Berkeley tunable far infrared laser spectrometers,” *Rev. Sci. Instrum.* **62**, 1701 (1991).
- ⁴⁸K. Liu, R. S. Fellers, M. R. Viant, R. P. McLaughlin, M. G. Brown, and R. J. Saykally, “A long path length pulsed slit valve appropriate for high temperature operation: Infrared spectroscopy of jet-cooled large water clusters and nucleotide bases,” *Rev. Sci. Instrum.* **67**, 410 (1996).
- ⁴⁹C. M. Western, “PGOPHER: A program for simulating rotational, vibrational, and electronic spectra,” *J. Quant. Spectrosc. Radiat. Transfer* **186**, 221 (2016).
- ⁵⁰V. Barone, “Anharmonic vibrational properties by a fully automated second-order perturbative approach,” *J. Chem. Phys.* **122**, 14108 (2005).
- ⁵¹V. Barone, “Vibrational zero-point energies and thermodynamic functions beyond the harmonic approximation,” *J. Chem. Phys.* **120**, 3059 (2004).
- ⁵²M. J. Frisch, G. W. Trucks, H. B. Schlegel, G. E. Scuseria, M. A. Robb, J. R. Cheeseman, G. Scalmani, V. Barone, B. Mennucci, G. A. Petersson, H. Nakatsuji, M. Caricato, X. Li, H. P. Hratchian, A. F. Izmaylov, J. Bloino, G. Zheng, J. L. Sonnenberg, M. Hada, M. Ehara, K. Toyota, R. Fukuda, J. Hasegawa, M. Ishida, T. Nakajima, Y. Honda, O. Kitao, H. Nakai, T. Vreven, J. A. Montgomery, Jr., J. E. Peralta, F. Ogliaro, M. Bearpark, J. J. Heyd, E. Brothers, K. N. Kudin, V. N. Staroverov, R. Kobayashi, J. Normand, K. Raghavachari, A. Rendell, J. C. Burant, S. S. Iyengar, J. Tomasi, M. Cossi, N. Rega, J. M. Millam, M. Klene, J. E. Knox, J. B. Cross, V. Bakken, C. Adamo, J. Jaramillo, R. Gomperts, R. E. Stratmann, O. Yazyev, A. J. Austin, R. Cammi, C. Pomelli, J. W. Ochterski, R. L. Martin, K. Morokuma, V. G. Zakrzewski, G. A. Voth, P. Salvador, J. J. Dannenberg, S. Dapprich, A. D. Daniels, Ö. Farkas, J. B. Foresman, J. V. Ortiz, J. Cioslowski, and D. J. Fox, GAUSSIAN 09, Revision D.01, Gaussian Inc., Wallingford, CT, 2009.
- ⁵³H. C. Longuet-Higgins, “The symmetry groups of non-rigid molecules,” *Mol. Phys.* **6**, 445 (1963).